

# Integrable Magnetless Thin Film Waveguide Optical Isolator based on Bismuth Iron Garnet Material

V. Stenger<sup>(1)</sup>, D. Karki<sup>(2)</sup>, A. Pollick<sup>(3)</sup>, M. Levy<sup>(2)</sup>

(1) SRICO, Inc., Columbus, Ohio 43235, USA, [vestenger@srico.com](mailto:vestenger@srico.com)

(2) Michigan Technological University, Houghton, Michigan 49931, USA

(3) SRICO, Inc., Columbus, Ohio 43235, USA

**Abstract:** A passive magnetless integrated optic Faraday isolator has been demonstrated that features ~3 dB total insertion loss and 25 dB isolation. The compact 500  $\mu\text{m}$  long ridge waveguide isolator is integrable with silicon photonic platforms.

## 1. Introduction

In optical circuits, isolators protect the laser source from back-reflected light originating downstream. Over the last several decades various research groups have investigated the on-chip integration of optical isolators, driven by the anticipated robustness, functional reliability, and fabrication economy of integrated circuits. A number of successes have been achieved in this pursuit [1-6]. These achievements have mostly focused on the implementation of on-chip prototypes based on magneto-optic (MO) Faraday or non-reciprocal-phase-shift (NRPS) effects, aimed at optimizing optical isolation and minimizing insertion losses [1-6]. An important feature that has not received as much attention has been downsizing the magnetizing element in most of these prototypes [3, 6, 8]. Permanent magnets or electro-magnets are used to saturate the magnetization in the MO films responsible for the nonreciprocal operation of these devices. They contribute a considerable fraction of the bulk in the optical isolator [1-3].

In this paper, we report an alternative technology to address the minimization of the bulk produced by the magnetizing element: eliminating it altogether, while retaining the MO functionality. This is realized through the incorporation of latching Faraday-rotator liquid-phase-epitaxial (LPE) iron-garnets into the isolator structure. The key to their bias-magnet-free operation resides in the composition of the garnet, achieved through the incorporation of europium in order to reduce the saturation magnetization of the garnet without creating a compensation point [7]. The nominal composition of the garnet is  $\text{Bi}_x(\text{Eu}_z\text{Ho}_{1-z})_{3-x}\text{Fe}_{5-y}\text{Ga}_y\text{O}_{12}$  per formula unit. Previous work on this material has shown the preservation of magnetization and 45° Faraday rotation with less than 0.1 dB insertion loss in these films down to 11  $\mu\text{m}$  thickness, fabricated by mechanical polishing [8].

## 2. Methodology

### 2.1. Sample Processing

Latching bismuth iron garnet samples were acquired commercially from II-VI, Inc. in the form of 10 mm x 10 mm x 480  $\mu\text{m}$  plates, magnetized perpendicular to the plate surface. The plates were anti-reflection coated, front and back, and delivered approximately 45° Faraday rotation in the telecom C-Band wavelength range. Two 30  $\mu\text{m}$  thick Polarcor™ polarizer films, polarization axes aligned at a 45° offset, were bonded on opposite faces of the latching MO iron garnet samples using benzocyclobutene (BCB). BCB represented a robust and foundry compatible process that could reliably withstand lapping and polishing processes without detaching the polarizers. Strips 0.5 mm wide x 10 mm x 480  $\mu\text{m}$  in size, were diced from the polarizer and iron garnet sample assembly, with the magnetization direction along the 480  $\mu\text{m}$  side. These strips were then thinned and polished, via a lapping and polishing process, to produce thin slab waveguides from 60  $\mu\text{m}$  down to 12  $\mu\text{m}$  in thickness and 10 mm x 480  $\mu\text{m}$  in size. Fig. 1 shows an example of a polished film with polarizers attached.

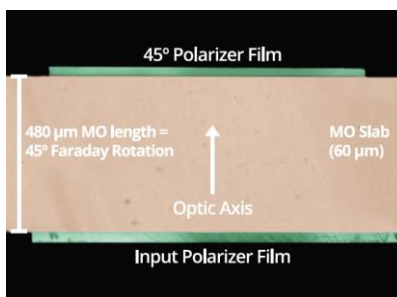


Fig. 1. Top view of a thin film slab waveguide isolator assembly with polarizers attached to the end facets.

## 2.2. Ridge Waveguide Faraday Isolator

Ridge waveguides, 12  $\mu\text{m}$  width and 3.6  $\mu\text{m}$  in depth, were patterned in a 12  $\mu\text{m}$  thin latching MO iron garnet film, with polarizers attached, by focused ion beam (FIB) milling. A scanning electron microscope image of the ridge waveguide structure is shown in Fig. 2. As can be seen in Fig. 2, the ridges were extended to include the polarizer film sections. Variation in the FIB removal rate caused a step in the etch depth at the polarizer/iron garnet interface. The process is currently being optimized to eliminate this step and improve overall fidelity of the end facets.

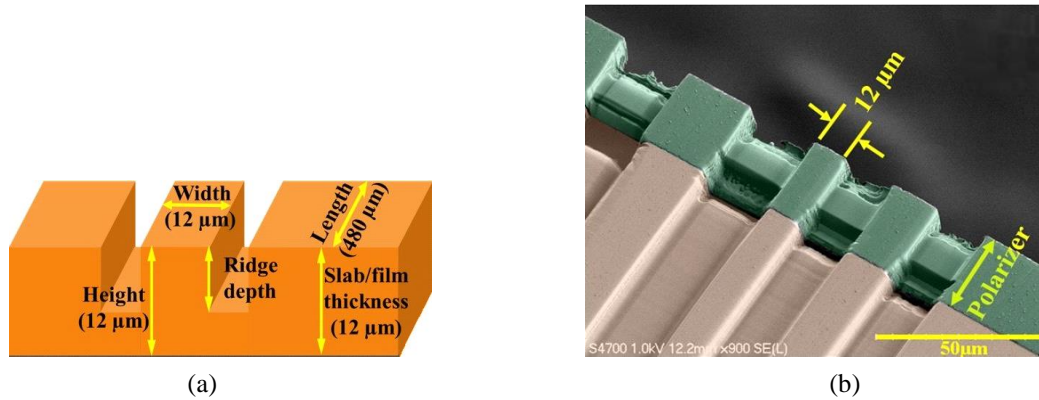


Fig. 2. (a) Geometry of the MO ridge waveguide and (b) SEM image of an end facet of the fabricated ridge waveguide isolator.

The fabricated ridge waveguide isolator may be integrated with other optoelectronic elements on a common silicon photonic platform using the same etched pocket, drop-in alignment and die bond attachment technique used to integrate III-V sources and detectors. The MO waveguides in this work were designed to match standard single mode fibers and, as such, are expected to couple efficiently to standard silicon photonic fiber edge coupler elements.

## 2.3. Optical Characterization

The optical test set-ups for slab and ridge waveguide isolator structures consisted of a fiber pig-tailed tunable C-Band laser source, polarization controller, a lensed fiber coupling linearly polarized light into the optical isolator structure, a Glan-Thomson polarizer to analyze the angular-dependence of the output polarization, and an optical power meter. The output profiles from 12  $\mu\text{m}$  thin slab and ridge waveguides were observed on a display screen connected to the IR camera. Fig. 3 shows typical transverse electric (TE) output mode profiles observed for the slab and ridge waveguide structures under study, as well as the simulated mode profile for the ridge waveguide.

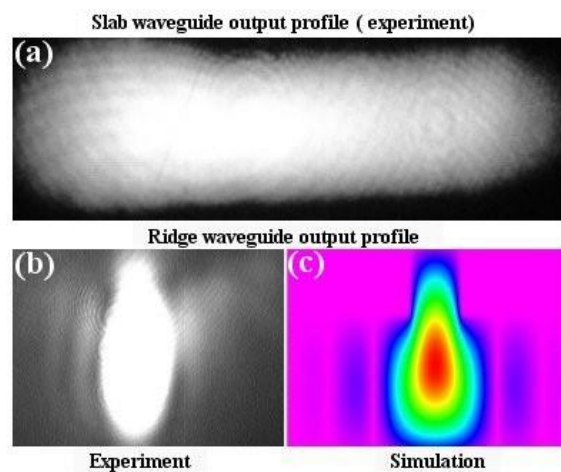


Fig. 3. IR camera images of output profiles observed for (a) slab waveguide and (b) ridge-waveguide. (c) Simulated fundamental mode profile for the ridge waveguide.

Optical isolation and insertion loss were measured between 1520 nm and 1580 nm. Transmitted power in the backward propagation direction divided by forward power through the device defines the optical isolation. Insertion

loss is defined as the transmitted power in the forward direction divided by the input power. Optical loss and isolation performances were measured both at the slab waveguide level and for the ridge waveguide. It was anticipated that the ridge guide would exhibit increased loss, relative to the slab, due to finite sidewall and end facet quality.

### 3. Test results

Optical test results for a 12  $\mu\text{m}$  thin film slab and the ridge waveguide isolator structures are shown in Fig. 4a and Fig. 4b, respectively. Relative to the ridge guide, the slab waveguide device can be seen to have overall higher isolation and lower loss. This difference in performance may be attributed to sidewall related scatter losses in the ridge guide. Effects of fiber mode mismatch can also increase for the ridge guide, relative to the slab guide, due to the increased degree of confinement. Even with these combined effects, the loss and isolation for the ridge waveguide device were about 3 dB and 25 dB, respectively.

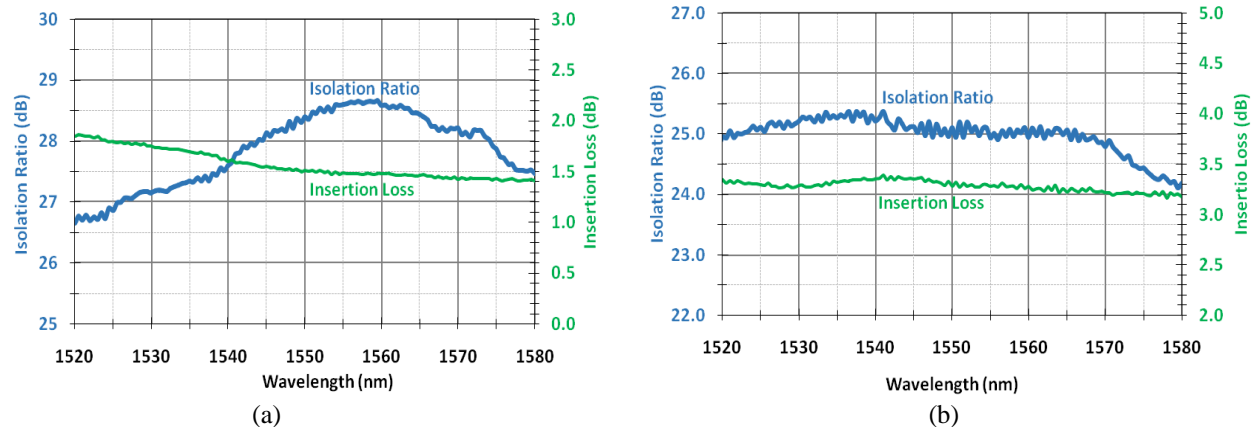


Fig. 4. Optical test results for the fabricated (a) 12  $\mu\text{m}$  slab waveguide and (b) ridge waveguide isolator structures.

For comparison, free space bulk isolators feature minimum isolation of 30 dB over the C-band, and maximum insertion loss of 0.5 dB. It is notable that the approximately 25 dB isolation in the single stage ridge guide is already approaching that for bulk isolators. Improved fabrication processes and mode matching are expected to further improve ridge guide isolation to 30 dB and insertion loss to less than 1 dB.

### 4. Conclusions

Magnetless thin film waveguide isolators have been demonstrated. A slab waveguide isolator exhibited 29 dB isolation and total insertion loss of 1.5 dB. A thin film ridge waveguide isolator exhibited 25 dB isolation and loss just over 3 dB, which included fiber mode mismatch losses. It is anticipated that improved fabrication and mode matching will produce ridge waveguide isolator devices with isolation of over 30 dB and loss less than 1 dB.

### 5. References

- [1] B. J. H. Stadler, and T. Mizumoto, "Integrated Magneto-Optical Materials and Isolators: A Review," *IEEE Photonics Journal*, 6, (1), 1-15 (2014).
- [2] M. Levy, "The On-Chip Integration of Magneto-optic Waveguide Isolators," *IEEE J. of Selected Topics in Quantum Electronics*, 8, (6), 1300-1306, (2002).
- [3] M. Levy, R. M. Osgood, Jr., H. Hegde, F. J. Cadieu, R. Wolfe, and V. J. Fratello, "Integrated Optical Isolators with Sputter-Deposited Thin-Film Magnets," *IEEE Phot. Technol. Lett.*, 8, (7), 903-905 (1996).
- [4] J. Fujita, M. Levy, R. M. Osgood, Jr., L. Wilkens, and H. Dötsch, "Waveguide Optical Isolator Based on Mach-Zehnder Interferometer," *Appl. Phys. Lett.*, 76, (16), 2158-2160 (2000).
- [5] L. Bi, J. Hu, P. Jiang, D. H. Kim, G. F. Dionne, L. C. Kimerling, C. A. and Ross, "On-chip Optical Isolation in Monolithically Integrated Nonreciprocal Optical Resonators," *Nature Photonics*, 5, 12, 758-762 (2011).
- [6] H. Lira, Z. Yu, S. Fan, and M. Lipson, "Electrically Driven Nonreciprocity Induced by Interband Photonic Transition on a Silicon Chip," *Phys. Rev. Lett.*, 109, (3) pp 033901 (2012).
- [7] R. R. Abbott, V. J. Fratello, S. J. Licht, and I. Mnushkina, "Article Comprising a Faraday Rotator that Does Not Require a Bias Magnet," US Patent 6770223 B1, August 2004.
- [8] D. Karki, V. Stenger, A. Pollick, and M. Levy, "Thin-Film Magnet-less Faraday Rotators for Compact Heterogeneous Integrated Isolators," *J. Appl. Phys.*, 121, (23), pp 233101 (2017).